JACC: BASIC TO TRANSLATIONAL SCIENCE VOL. 4, NO. 8, 2019
© 2019 THE AUTHORS. PUBLISHED BY ELSEVIER ON BEHALF OF THE AMERICAN COLLEGE OF CARDIOLOGY FOUNDATION. THIS IS AN OPEN ACCESS ARTICLE UNDER THE CC BY-NC-ND LICENSE (http://creativecommons.org/licenses/by-nc-nd/4.0/).

PRECLINICAL RESEARCH

Seipin Knockout Mice Develop Heart Failure With Preserved Ejection Fraction

Bo Bai, PhD,[a,b] Wulin Yang, PhD,[c,d] Yanyun Fu, PhD,[a] Hannah Lee Foon, SWA, PhD,[e] Wan Ting Tay, MAppStat,[f] Kangmin Yang, PhD,[b] Cuiting Luo, BS,[b] Jayantha Gunaratne, PhD,[e] Philip Lee, PhD,[a] Michael R. Zile, MD,[g,h] Aimin Xu, PhD,[b,i] Calvin W.L. Chin, MD, PhD,[f] Carolyn S.P. Lam, MD, PhD,[f] Weiping Han, PhD,[a] Yu Wang, PhD[b]

VISUAL ABSTRACT

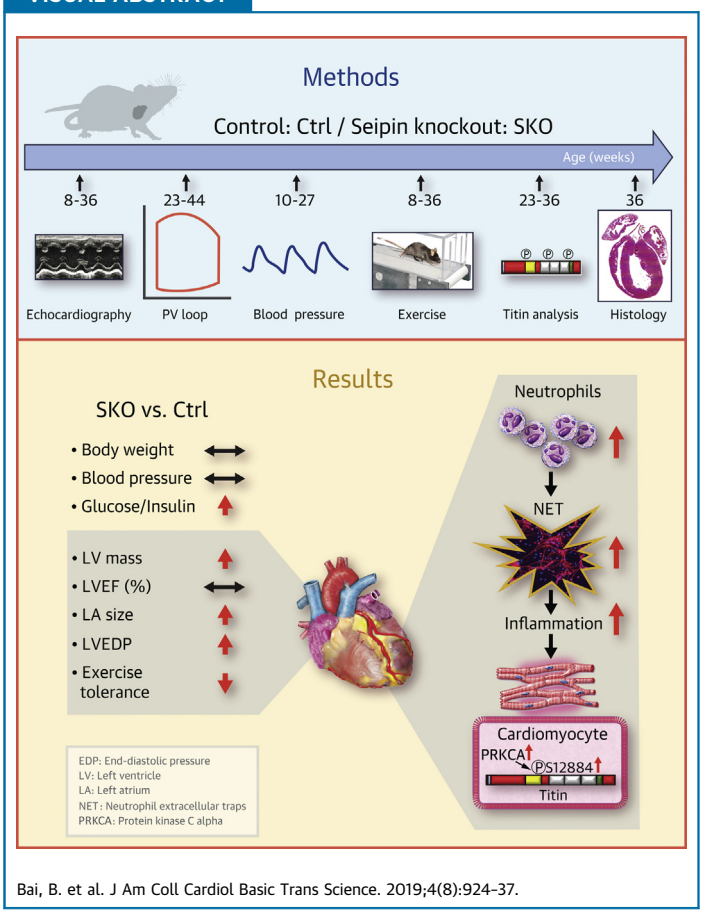

Bai, B. et al. J Am Coll Cardiol Basic Trans Science. 2019;4(8):924–37.

HIGHLIGHTS

- **The lean diabetic SKO mouse represents a novel and validated murine model of HFpEF.**
- **The SKO HFpEF mouse model recapitulates the cardiac structure and function abnormalities in lean diabetic HFpEF patients in Asia.**
- **Altered cellular titin phosphorylation and increased extracellular interstitial fibrosis associated with neutrophil extracellular traps contribute to the left ventricular stiffness.**
- **Metabolic disturbances arising from insulin resistance and diabetes in the absence of hypertension or obesity may lead to HFpEF.**

ISSN 2452-302X https://doi.org/10.1016/j.jacbts.2019.07.008

SUMMARY

The lean diabetic patients with heart failure with preserved ejection fraction (HFpEF) in Asia suffer from adverse clinical outcomes and poor life quality. The suitable animal models are urgently needed for mechanistic study and therapeutic innovations. Our study reports that lipodystrophic mice with seipin depletion are lean, diabetic, and recapitulate major manifestations of clinical HFpEF, thereby clarifying that lean diabetes per se may produce HFpEF characteristics. We further demonstrate that increased cardiac titin phosphorylation and reactive interstitial fibrosis associated with neutrophil extracellular traps lead to left ventricular stiffness and suggest that both pathways may be potential therapeutic targets in Asian HFpEF patients.
(J Am Coll Cardiol Basic Trans Science 2019;4:924–37) © 2019 The Authors. Published by Elsevier on behalf of the American College of Cardiology Foundation. This is an open access article under the CC BY-NC-ND license (http://creativecommons.org/licenses/by-nc-nd/4.0/).

ABBREVIATIONS AND ACRONYMS

Ctrl = control (mice)

EDPVR = end-diastolic pressure-volume relationship

HFpEF = heart failure with preserved ejection fraction

IQR = interquartile range

LA = left atrial

LV = left ventricular

NET = neutrophil extracellular trap

PEVK = proline, glutamate, valine, and lysine

SKO = seipin knockout

Heart failure with preserved ejection fraction (HFpEF) has been described as the greatest unmet need in cardiovascular medicine today (1). It constitutes the dominant form of HF in aging societies, is the top cause of hospitalization among elderly persons worldwide, and carries a dismal prognosis with >50% 5-year mortality (2). Outcomes have not been improved over the last decades, and there is currently still no effective therapy proven to improve survival in HFpEF (2). There is an urgent need to better understand the pathophysiology of HFpEF and identify potential novel therapeutic targets (3).

HFpEF represents a broad cohort of patients with a range of comorbidities, such as hypertension, obesity, and diabetes, that requires individualized management based on biological phenotypes (4,5). However, recent epidemiologic data from Asia suggest a unique lean diabetic phenotype of HFpEF, compared with other HF phenotypes, has the worst quality of life, more severe signs and symptoms of HF, and the highest rate of adverse clinical outcomes (6–8).

SEE PAGE 938

A critical obstacle to therapeutic innovation in HFpEF has been the absence of suitable animal models that accurately recapitulate the complexities of the human disease (9,10). An ideal HFpEF animal model that captures 2 or more HFpEF features (e.g., concentric hypertrophy, diastolic dysfunction, and impaired exercise capacity) would be more helpful in providing mechanistic insights and therapeutic

From the [a]Singapore Bioimaging Consortium, Agency for Science, Technology and Research, Singapore; [b]State Key Laboratory of Pharmaceutical Biotechnology and Department of Pharmacology and Pharmacy, The University of Hong Kong, Hong Kong, China; [c]Anhui Province Key Laboratory of Medical Physics and Technology, Center of Medical Physics and Technology, Hefei Institutes of Physical Science, Chinese Academy of Sciences, Hefei, China; [d]Hefei Cancer Hospital, Chinese Academy of Sciences, Hefei, China; [e]Translational Biomedical Proteomics, Institute of Molecular and Cell Biology, Agency for Science, Technology and Research, Singapore; [f]National Heart Centre Singapore and Duke-National University of Singapore, Singapore; [g]Division of Cardiology, Department of Medicine, Medical University of South Carolina, Charleston, South Carolina; [h]Ralph H. Johnson Department of Veterans Affairs Medical Center, Charleston, South Carolina; and the [i]Department of Medicine, The University of Hong Kong, Hong Kong, China. This work is support by the Agency for Science, Technology and Research Biomedical Research Council, Bayer and the Asian neTwork for Translational Research and Cardiovascular Trials (ATTRaCT) Biomedical Research Council program (SPF2014/001, SPF2013/002, SPF2014/003, SPF2014/004, SPF2014/005); Research Grant Council grants (17121714) and Collaborative Research Funds (C7055-14G) of Hong Kong; the U.S. National Institutes of Health grants (1R01HL123478-01A1, NIH-NHLBI); and the Asian Sudden Cardiac Death in Heart Failure (ASIAN-HF) study is further supported by grants from Boston Scientific Investigator Sponsored Research Program, National Medical Research Council Singapore (R-172-003-219-511), and Bayer. Dr. Lam is supported by a Clinician Scientist Award from the National Medical Research Council of Singapore; has received research support from Boston Scientific, Bayer, Roche Diagnostics, AstraZeneca, Medtronic, and Vifor Pharma; has served as consultant or on the Advisory Board/Steering Committee/Executive Committee for Boston Scientific, Bayer, Roche Diagnostics, AstraZeneca, Medtronic, Vifor Pharma, Novartis, Amgen, Merck, Janssen Research & Development LLC, Menarini, Boehringer Ingelheim, Novo Nordisk, Abbott Diagnostics, Corvia, Stealth BioTherapeutics, JanaCare, Biofourmis, Darma, Applied Therapeutics, MyoKardia, WebMD Global LLC, Radcliffe Group Ltd and Corpus;and participated on behalf of the ASIAN-HF investigators. All other authors have reported that they have no relationships relevant to the contents of this paper to disclose. Membership of ASIAN-HF authors is provided in the Supplemental Appendix.

The authors attest they are in compliance with human studies committees and animal welfare regulations of the authors' institutions and Food and Drug Administration guidelines, including patient consent where appropriate. For more information, visit the *JACC: Basic to Translational Science* author instructions page.

Manuscript received May 27, 2019; revised manuscript received July 15, 2019, accepted July 16, 2019.

FIGURE 1 The Development of Cardiomegaly in the Lean Diabetic SKO Mice

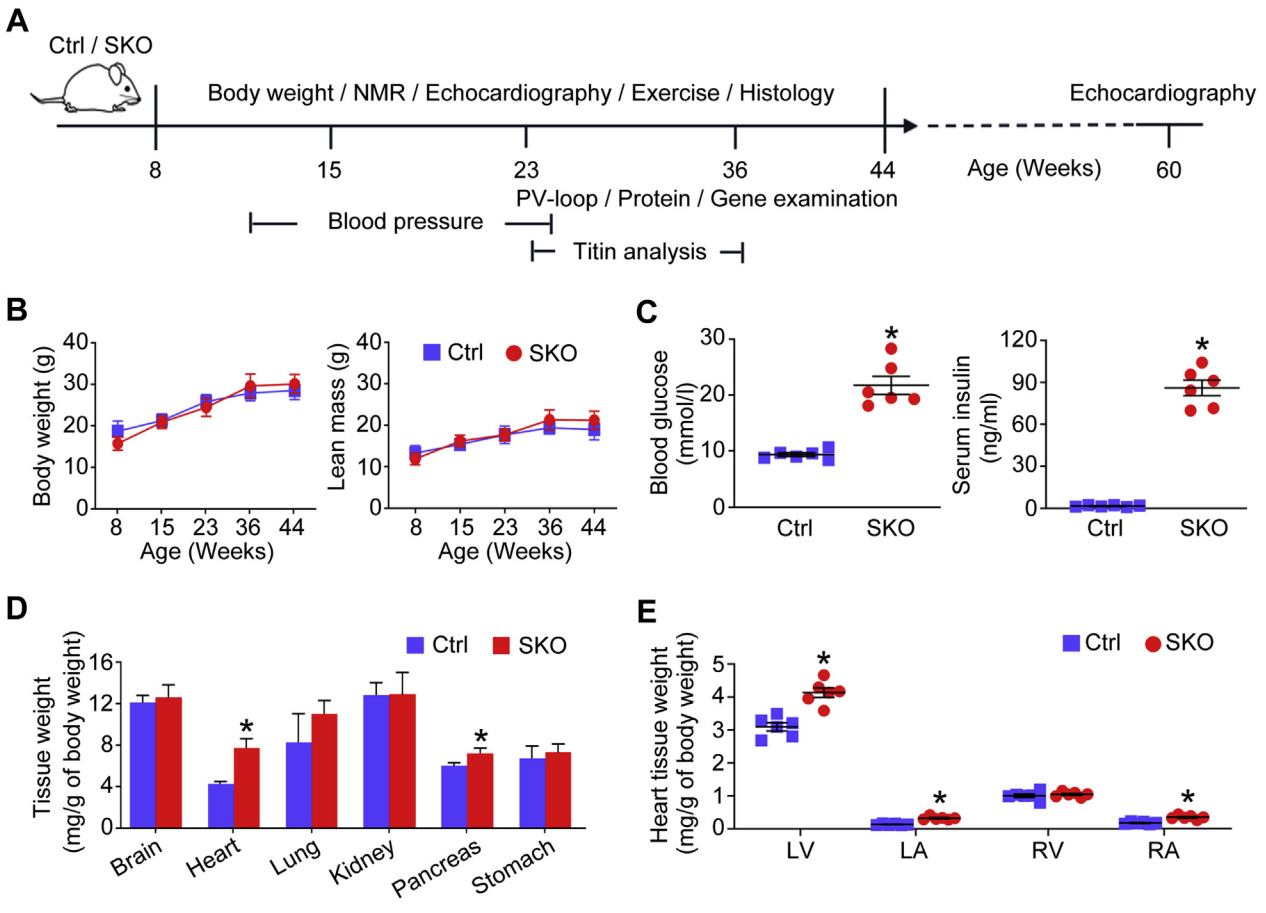

Mice were subjected to phenotypic characterizations according to the protocol **(A)** and nuclear magnetic resonance (NMR) **(B)** to measure body weight and lean mass. **(C)** Blood glucose and serum insulin of mice (18 to 24 weeks old) under basal feeding; **(D)** the ratio between tissue weight and body weight of mice (~24 weeks old); and **(E)** the ratio of left ventricular (LV), left atrial (LA), right ventricular (RV), and right atrial (RA) weight to body weight of mice (41 to 46 weeks old) were analyzed. *$p < 0.05$, compared with control (Ctrl) mice ($n = 6$). PV = pressure-volume; SKO = seipin knockout.

innovations (9,10). So far, such ideal animal models, which show the effect of lean diabetes on the onset of HFpEF, remain absent.

Lipodystrophies are clinical disorders characterized by the selective loss of adipose tissue and severe insulin resistance, leading to diabetes (11,12). Notably, the common cardiac abnormality, hypertrophic cardiomyopathy, occurs with considerable frequency in cohort patients with lipodystrophy caused by different genetic defects (13-15). Patients carrying Berardinelli-Seip congenital lipodystrophy-2 (BSCL2)/seipin mutation exhibit the most severe lipodystrophic phenotype (11,16), and they are lean, diabetic, and exhibit left ventricular (LV) hypertrophy without reduction of EF (13,15). The mechanisms underlying these cardiac manifestations remain poorly understood.

In the current study, we aimed to study whether aged seipin knockout (SKO) mice may serve as a validated model of lean diabetic HFpEF and to investigate potential pathophysiologic pathways underlying LV structural-functional abnormalities in the model.

METHODS

MICE AND STUDY DESIGN. The generation of SKO and littermate control (Ctrl) mice was described previously (17). The timeline to investigate the metabolic, cardiac, and exercise characteristics of male mice is shown in Figure 1A. All animal care and experimental procedures were approved by the Committee on the Use of Live Animals for Teaching and Research of the University of Hong Kong and the

Institutional Animal Care and Use Committee of the Agency for Science, Technology, and Research and were carried out in accordance with the *Guide for the Care and Use of Laboratory Animals, Eighth Edition*, published by the U.S. National Institutes of Health. The Supplemental Appendix contains additional Methods and Materials.

HUMAN STUDY POPULATION AND DESIGN. The human data were collected from the ASIAN-HF (Asian Sudden Cardiac Death in Heart Failure) registry. The prospective study design of the ASIAN-HF registry was published previously (8,18,19). The ethics approvals, study definitions, clinical outcomes, echocardiography, and imaging collection were described in detail (8). In the current study, we further analyzed and compared data from lean diabetic HFpEF patients and age-matched control subjects without HF from the community.

STATISTICAL ANALYSIS. For animal studies, all calculations were performed using SPSS software (version 19.0; IBM Corporation, Armonk, New York). Results are presented as mean ± SEM. Student's *t*-test for unpaired observations or one-way analysis of variance with Bonferroni correction for multiple comparisons was performed to analyze the statistical differences between different groups. For all statistical comparisons, p values < 0.05 indicated statistical significance. For the human cohort study, data are given as means ± SD, medians and interquartile ranges (IQR) (25th and 75th percentiles), or numbers and proportions, as appropriate. Depending on the types of data, Student's *t*-test, Wilcoxon rank sum test, or chi-square test for unpaired observations was applied and p values < 0.05 indicated statistical significance. In addition, lean diabetic HFpEF patients were matched to community control subjects without HF with the same age where possible. Otherwise, the next closest age was used.

RESULTS

LEAN AND DIABETIC SKO MICE DEVELOP CARDIOMEGALY. SKO mice developed lipodystrophy after birth (17), but had similar body weight and lean mass as the Ctrl mice (**Figure 1B**). The adult SKO mice (18 to 24 weeks old) showed significantly elevated blood glucose and serum insulin levels under basal feeding (**Figure 1C**), which also displayed glucose intolerance and reduced insulin sensitivity (17). Moreover, we observed cardiomegaly in adult SKO mice (7.7 vs. 4.3 mg/g of body weight for SKO vs. Ctrl mice, ~24 weeks old) (**Figure 1D**). The ratios of LV, left atrial (LA), and right atrial weight to body weight were significantly higher in SKO mice ages 41 to 46 weeks than in Ctrl mice of similar ages (**Figure 1E**). To clarify whether cardiomegaly was caused by the seipin mutation in mouse heart tissues, we first profiled *Bscl2* messenger ribonucleic acid level in mouse tissues. In Ctrl mice, the *Bscl2* gene was abundantly expressed in adipose tissues. By contrast, its expression level was the lowest in mouse hearts and muscles (Supplemental Figure 1A). As expected, *Bscl2* expression was not detectable in SKO mouse tissues (Supplemental Figure 1A). We then established cardiomyocyte-specific SKO. We did not observe any difference in terms of ratios between heart tissue weight and tibia length, including LV, LA, right ventricular, and right atrial tissues, between cardiomyocyte-specific SKO mice ages 55 to 60 weeks and corresponding Ctrl mice of similar ages (Supplemental Figure 1B). These data suggest that cardiac abnormalities of SKO mice were unlikely to be the result of seipin mutation in mouse hearts, but were more likely due to systematic factors (e.g., hyperglycemia).

SKO MICE EXHIBIT LV CONCENTRIC HYPERTROPHY WITHOUT HYPERTENSION. We performed echocardiography in the SKO and Ctrl mice and found thickened LV walls and increased LV mass, that is, cardiac hypertrophy in the SKO mice. These differences became even more prominent with aging (**Figure 2A**). By contrast, the LV internal diameter was comparable between the 2 groups of mice (**Figure 2A** and Supplemental Figure 2A). In addition, adult SKO mice (~36 weeks old), compared with their Ctrl mice, had higher heart weight to tibia length ratio, greater whole heart cross-sectional area as well as cardiomyocyte enlargement (**Figure 2B**). Notably, SKO mice exhibited preserved LVEF and fractional shortening (**Figure 2A**), even in mice ~60 weeks old (Supplemental Figure 2B). We next examined gene expression of cardiac hypertrophy markers, including alpha-skeletal actin (*Acta1*) and atrial natriuretic peptide (*Nppa*) (20). Both *Acta1* and *Nppa* were significantly up-regulated in heart tissues of adult SKO mice (~36 weeks old). Induction of *Nppa* and *Acta1* genes is dependent on the activation of signal transducer and activator of transcription 3 (STAT3) (21–23). Consistently, we found hyperphosphorylation of STAT3 and its upstream Janus kinase 2 (JAK2) in heart tissues of SKO mice (**Figures 2C and 2D**). Although SKO mice developed LV concentric hypertrophy with aging, the systolic and diastolic arterial blood pressure collected during the dark cycle (from 7 PM to 7 AM) was comparable between SKO and their Ctrl mice (**Figure 2E**).

SKO MICE EXHIBIT LV DIASTOLIC DYSFUNCTION, EXERCISE INTOLERANCE, AND LA ENLARGEMENT. We assessed both components of LV diastolic

FIGURE 2 The Concentric LV Hypertrophy in the Absence of Hypertension in the SKO Mice

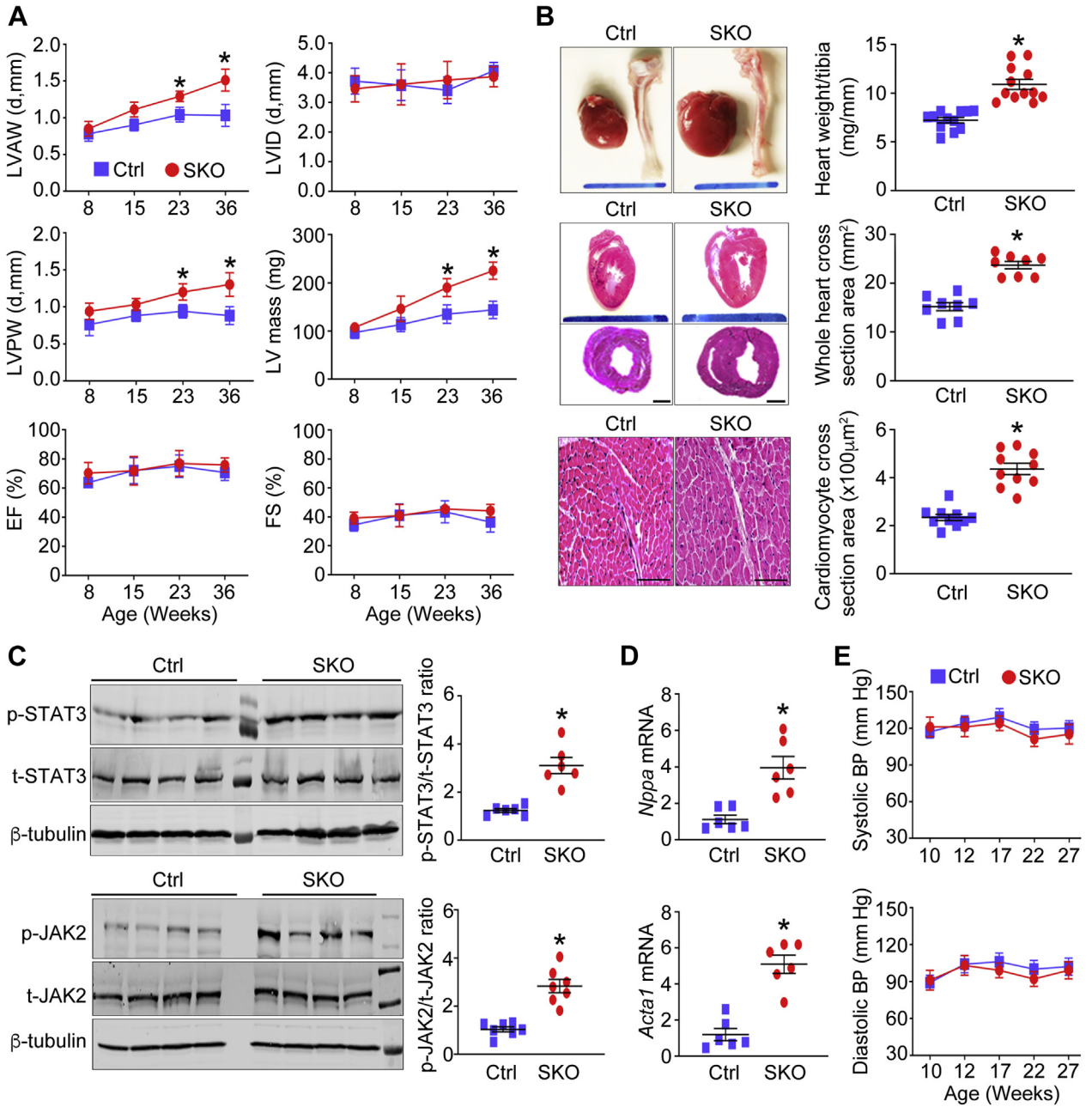

(A) At 8, 15, 23, and 36 weeks of age, mice were subjected to echocardiography to measure the thickness of the left ventricle anterior wall (LVAW) and left ventricle posterior wall (LVPW), left ventricle internal diameter (LVID) in diastole (d), LV mass, ejection fraction (EF), and fractional shortening (FS) (n = 8 to 10). **(B)** The heart tissues of adult mice (36 weeks old) were subjected to examine the ratio of heart weight to tibia length (scale bar = 10 mm, n = 12). Representative images of hematoxylin and eosin-stained heart sections (**top,** longitudinal section, scale bar = 10 mm; **bottom,** horizontal section, scale bar = 1 mm) were shown. The cross-sectional area of whole heart tissues (n = 8) and cardiomyocytes (scale bar = 100 μm, n = 10) was quantified in each group of mice. **(C)** The total (t) and phosphorylated **(p)** signal transducer and activator of transcription 3 (STAT3) and Janus kinase 2 (JAK2) were examined by Western blotting (n = 6), and **(D)** the gene expression of hypertrophic markers, including atrial natriuretic peptide (*Nppa*) and alpha-skeletal actin (*Acta1*), were detected using mouse heart tissues (n = 6). Fold change was calculated for comparison. **(E)** Blood pressure (BP) of mice was collected by telemetry system during the dark cycle (from 7 PM to 7 AM, n = 3). *$p < 0.05$, compared with Ctrl mice. mRNA = messenger ribonucleic acid; other abbreviations as in Figure 1.

FIGURE 3 LV Diastolic Dysfunction, Exercise Intolerance, and LA Enlargement in the SKO Mice

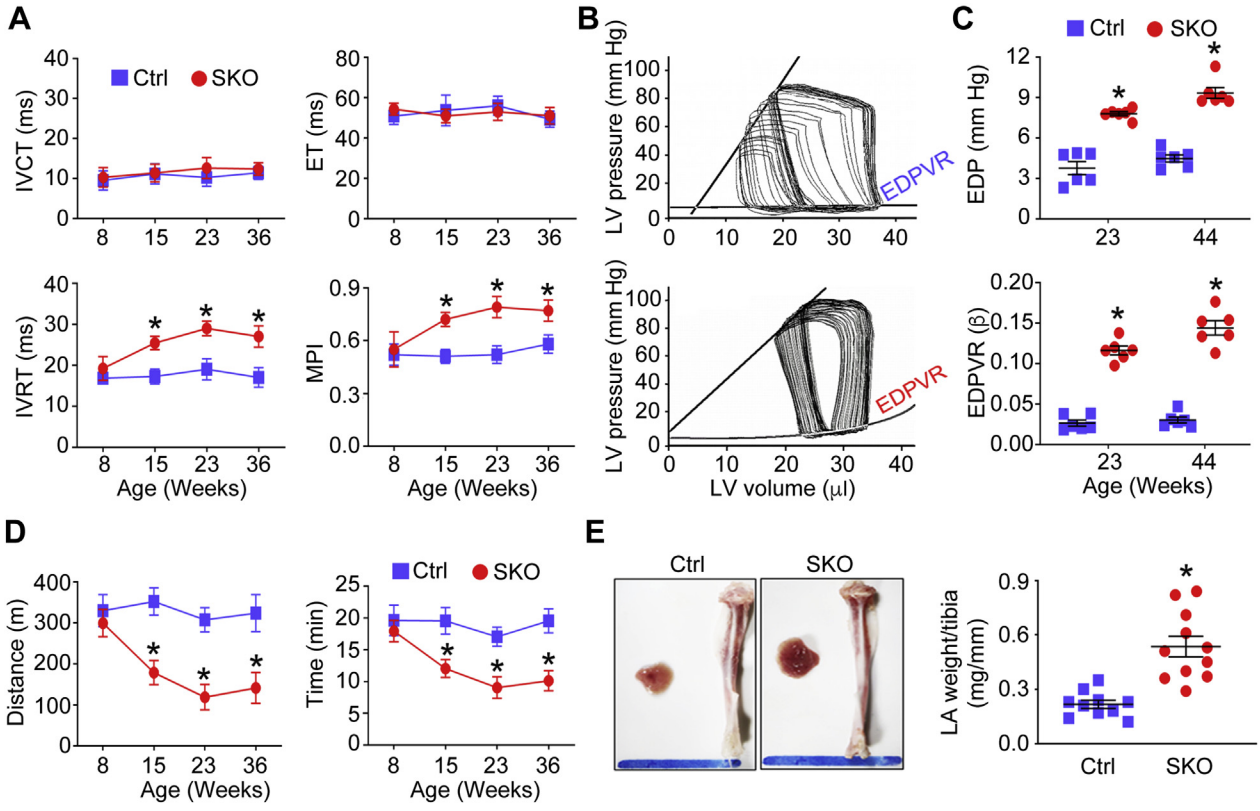

(A) The Doppler echocardiography was used to examine LV isovolumic contraction time (IVCT) and isovolumic relaxation time (IVRT), ejection time (ET), and myocardial performance index (MPI) (n = 8 to 10). The LV pressure-volume loops were analyzed to show representative examples of pressure-volume loops of mice (23 weeks old) **(B)** and measure LV end-diastolic pressure (EDP) and diastolic stiffness coefficient β derived from the end-diastolic pressure-volume relationship (EDPVR) of mice (n = 6) **(C). (D)** Mouse running distance and time via treadmill running test (n = 6); **(E)** the histology of LA tissues and ratio of LA weight to tibia length of mice (36 weeks old) were examined (scale bar = 10 mm, n = 10 to 11). *p < 0.05, compared to Ctrl mice. Abbreviations as in Figure 1.

function as mice aged: 1) active LV relaxation (isovolumic relaxation time); and 2) passive LV diastolic stiffness (end-diastolic pressure-volume relationship [EDPVR]). There was no difference in isovolumic contraction time or ejection time between SKO and Ctrl mice. In contrast, prolonged isovolumic relaxation time, indicative of impaired LV relaxation, was developed in SKO mice, compared with the Ctrl mice, beginning in young adulthood (~15 weeks old). The difference became more apparent with aging (Figure 3A). Moreover, prolonged isovolumic relaxation time contributed to worsening myocardial performance index (higher values indicating worse performance) with age in SKO mice (Figure 3A) (24). LV PV loop analysis showed steeper EDPVR in adult SKO mice compared with in Ctrl mice (23 weeks old) (Figure 3B). Accordingly, LVEDP was significantly increased in adult SKO mice (23 weeks old), and the differences became more prominent in older mice (44 weeks old) (Figure 3C). Meanwhile, the diastolic stiffness coefficient β derived from EDPVR was steadily higher in SKO mice (Figure 3C). Similar to Asian HFpEF patients that exhibited reduced exercise tolerance (6), when compared with the Ctrl group, SKO mice displayed exercise intolerance (reduced running distance and running time) beginning in young adulthood (~15 weeks old)(Figure 3D). Consistent with compromised diastolic function, the LA size and weight of SKO mice (~36 weeks old) were significantly increased (Figure 3E).

CARDIAC TITIN PHOSPHORYLATION IS ALTERED IN SKO MYOCARDIUM. To explore the underlying mechanisms for increased LV diastolic stiffness in SKO mice, we first investigated the total expression and phosphorylation of titin in LV tissues of adult mice (23 to 36 weeks old). Using agarose gel electrophoresis, we found no significant changes of total titin expression relative to myosin heavy chain in LV

FIGURE 4 Altered Cardiac Titin Phosphorylation in the SKO Mice

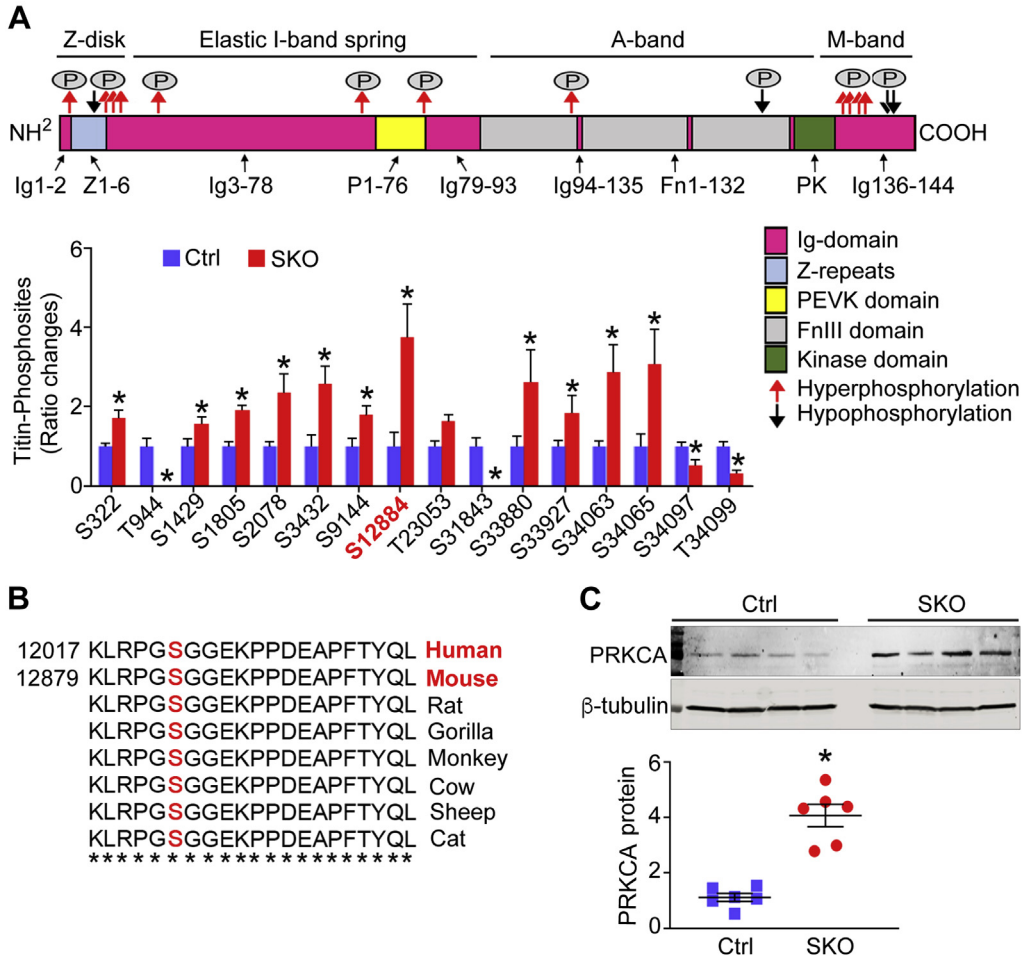

(A) The quantitative mass spectrometry was used to measure ratio changes of titin phosphosites of mouse LV tissues (23 to 36 weeks old, n = 6). The **bold line arrows (red and black)** indicate localization of changed phosphosites in the canonical sequence of mouse titin (UniProtKB entry A2ASS6). **(B)** Multiple sequence alignments showed serine (S) 12884 of murine cardiac titin was a conserved residue. **(C)** Protein expression of protein kinase C alpha (PRKCA) was examined in mouse heart tissues (23 to 36 weeks old, n = 6). Fold change was calculated for comparison. *p < 0.05, compared with Ctrl mice FnIII = fibronectin type III domain; Ig = immunoglobulin-like; PEVK = proline, glutamate, valine, and lysine; T = threonine. Abbreviations as in Figure 1.

myocardium, comparing between SKO and Ctrl mice (Supplemental Figure 3). We then examined titin phosphorylation—a crucial mechanism responsible for increased myocardial stiffness in clinical HFpEF (25). We used quantitative mass spectrometry to detect titin phosphorylation. A total of 238 titin phosphosites was quantified (localization probability $\acute{\imath} > 0.9$). An intensity ratio of SKO versus Ctrl phosphorylation was obtained for 46 titin phosphosites, among which 30 were similar, but 16 were differentially phosphorylated between the 2 groups, with the SKO-Ctrl ratio ≤0.5 or ≥1.5 indicating as hypo phosphorylated or hyperphosphorylated residues in SKO mice compared with Ctrl mice. These sites were marked in the canonical domain sequence of mouse titin according to UniProtKB entry A2ASS6 (UniProt Consortium, Hinxton, Cambridge, United Kingdom) (**Figure 4A**). Most of the sites shared similar amino acid sequences with human titin (entry Q8WZ42) (Supplemental Figure 4). Two phosphosites were undetectable in SKO hearts: 1) threonine 944 between Z-repeat 6 and immunoglobulin-like domain 3 of the Z-disk region; and 2) serine 31843 at the fibronectin type-III domain 126 of the A-band region. Phosphorylation of serine 34097 and threonine 34099 in the M-band region was significantly down-regulated in the

SKO mouse hearts (Figure 4A). By comparison, 12 titin phosphosites were hyperphosphorylated in the SKO myocardium from Z-disk and E-, A-, and M-band regions. We found 2 hyperphosphorylated serine 322 and serine 1429 located within ZIS1 and ZIS5 regions of the Z-disk band, which contained multiple SPXR consensus motif repeats. Importantly, when focusing on the elastic I-band spring element, striking hyperphosphorylation of titin at serine 12884 (SKO-Ctrl ratio >3.5) was identified in SKO myocardium (Figure 4A). This phosphosite localized at the COOH-terminus of the titin region rich in proline, glutamate, valine, and lysine (PEVK domain) and was evolutionarily conserved across species (orthologous residue of serine 12022 of human titin at PEVK31) (Figure 4B). Hyperphosphorylation of titin at serine 12022 (serine 12884 in mouse) was previously identified in human failing hearts (26) and reported to increase myocardial stiffness in mouse and pig hearts (27,28). SKO hearts had elevated protein expression of protein kinase C alpha (PRKCA) (Figure 4C), an upstream kinase responsible for the phosphorylation of titin at serine 12884 (27,28). Conversely, we did not detect any difference in protein levels of cyclic guanosine monophosphate-dependent protein kinase (PRKG), cyclic adenosine monophosphate-dependent protein kinase catalytic, alpha (PRKACA), or extracellular signal-regulated protein kinases 1 and 2 (Erk1/2) in heart tissues of the 2 groups of mice (Supplemental Figure 5). Consistently, the cyclic adenosine monophosphate-dependent protein kinase, PRKG, or Erk1/2-dependent phosphorylation at the titin transcript variant N2-B (N2B) unique sequence of titin (N2-Bus) was not changed in LV tissues of the 2 groups of mice (Figure 4A).

SKO MOUSE MYOCARDIUM EXHIBITS REACTIVE INTERSTITIAL FIBROSIS ASSOCIATED WITH INFLAMMATION AND MASSIVE NEUTROPHIL INFILTRATION. Next, we investigated cardiac interstitial fibrosis, another hallmark seen in HFpEF patients that independently predicts intrinsic LV stiffness (25,29). The cardiac fibrosis was increased in SKO mice, compared with Ctrl mice, from young adulthood (~15 weeks old) and progressed with age (Figure 5A). Progression of cardiac fibrosis also coincided with increased gene expression of collagen 1 (*Col1a1*), interleukin 6 (*Il6*), and intercellular adhesion molecule 1 (*Icam1*), as well as augmented protein levels of tumor necrosis factor (TNF) in whole heart tissues of SKO mice (~24 weeks old) (Figures 5A and 5B). Meanwhile, several key markers reflecting activation of quiescent fibroblasts such as alpha-smooth muscle actin (ACTA2) (30) and transforming growth factor beta family (TGFB) (31) were significantly increased in hearts of adult SKO mice (~24 weeks old) (Figure 5B). The cardiac inflammation and interstitial fibrosis were associated with massive neutrophil infiltration in SKO myocardium, which also started from young ages (Figure 5C). To address the implication of infiltrated neutrophils in cardiac damage, we examined whether neutrophil extracellular traps (NET) were formed in SKO mouse hearts. The presence of NET was shown as intact neutrophils with condensed nuclei in SKO mouse hearts from a young age (15 weeks old) and persisted as large amorphous extracellular structures, released deoxyribonucleic acid fibers decorated with myeloperoxidase and citrullinated histone (32), in hearts of adult SKO mice (32 weeks old) (Figure 5D). Consistent with the formation of NET, the protein level of citrullinated histone 3, a well-recognized NET marker (33), was significantly elevated in SKO mouse hearts (24 to 30 weeks old) (Figure 5E).

SKO MICE SHARE MAJOR HFpEF CHARACTERISTICS WITH LEAN DIABETIC PATIENTS. The pan-Asian HF prospective study identified distinct lean diabetic HFpEF patients who had a strikingly high prevalence of diabetes (8). Compared with age-matched non-HF control subjects from the community, lean diabetic HFpEF patients were older, but had the comparable systolic blood pressure and body mass index. Among echocardiographic variables, lean diabetic HFpEF patients displayed nondilated concentric hypertrophy, which was evidenced by increased LV mass but normal LV volume. Despite the preserved LVEF, HFpEF patients showed apparent diastolic dysfunction, LA dilatation, as well as significantly reduced exercise tolerance (Table 1). Moreover, cardiovascular cardiac magnetic resonance in a subset of 54 lean diabetic HFpEF patients showed increased extracellular volume (median [IQR]: 30% [28, 33]), compared with healthy control subjects with normal values (median: 25% to 26%) regardless of age and sex, indicating the presence of LV fibrosis (34,35). Taken together, the major clinical characteristics of lean diabetic HFpEF patients were captured by the SKO mice.

DISCUSSION

We provide detailed cardiac phenotypic characterizations of SKO mice. The results demonstrate that lean diabetic SKO mice recapitulate multiple clinical characteristics of HFpEF, particularly those observed in lean diabetic Asian patients (Table 1). Both altered cardiac titin phosphorylation and increased LV

FIGURE 5 LV Reactive Interstitial Fibrosis and Neutrophil Infiltration in the SKO Mouse Myocardium

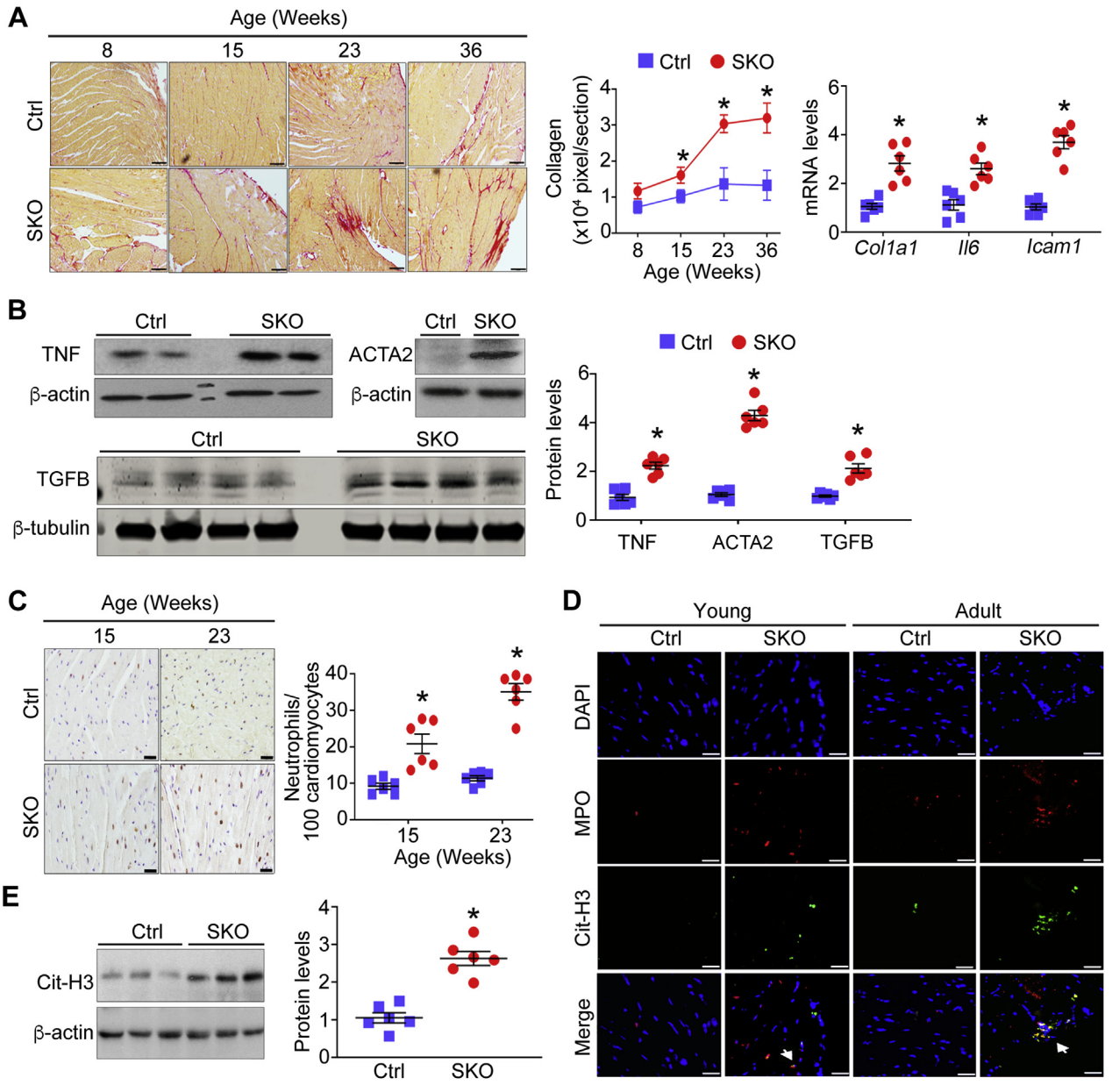

(A) Representative photomicrographs of picrosirius red staining of mouse heart tissues (scale bar = 100 μm). The pixel area of fibrosis was quantified in each group (n = 6). Gene expression of collagen 1 (*Col1a1*), interleukin 6 (*Il6*), and intercellular adhesion molecule 1 (*Icam1*), and **(B)** protein levels of alpha-smooth muscle actin (ACTA2), transforming growth factor beta family (TGFB), and tumor necrosis factor (TNF) were examined in mouse hearts (~24 weeks old, n = 6). Fold change was calculated for comparison. **(C)** Infiltrated neutrophils with positive immunohistochemical staining of antineutrophil-specific elastase were counted in mouse heart sections (scale bar = 20 μm, n = 6). **(D)** Representative images of in situ neutrophil extracellular traps in mouse hearts were indicated by **arrows** to show colocalization of deoxyribonucleic acid (4′,6-diamidino-2-phenylindole [DAPI], **blue**), myeloperoxidase ([MPO], **red**), and citrullinated histone 3 ([Cit-H3], **green**) (scale bar = 20 μm). **(E)** The protein level of Cit-H3 was examined in mouse heart tissues (24 to 30 weeks old, n = 6). Fold change was calculated for comparison. *$p < 0.05$, compared with Ctrl mice. Abbreviations as in Figure 1.

interstitial fibrosis may lead to intrinsic LV stiffness (Figure 6). Our murine HFpEF model is unique and significant with the following features: 1) diabetic animal without excessive weight gain; 2) concentric LV hypertrophy, LV diastolic dysfunction, and LA dilatation, associated with exercise intolerance and raised natriuretic peptides, recapitulating human HFpEF; 3) the LV hypertrophy occurred without an increase in blood pressure; 4) the intrinsic HFpEF features are advantageous for its utility as a preclinical model, in that the model overcomes problems of acute surgery insult, sudden onset of HF, deterioration of the LV systolic function, as well as the oncogenic response of existing animal models (9,10). As such, aged mice represent an ideal model of lean diabetic HFpEF, which allows us to continue mechanistic investigations through the multiorgan system and test novel therapeutic interventions, which are difficult to be carried out in human patients.

TITIN HYPERPHOSPHORYLATION AND INTERSTITIAL FIBROSIS CONTRIBUTE TO DIASTOLIC STIFFNESS IN THE SKO MICE. We unraveled that the post-translational modification of titin and increased interstitial fibrosis contributed to the diastolic stiffness of SKO mice, both of which are likely driven by the hyperglycemia. First, evidence linking altered titin phosphorylation with HF has been proposed in HFpEF patients (25). Recent studies have highlighted the importance of residues within the PEVK domain and N2-Bus as key targets of protein kinases in the regulation of titin mechanical function (36). Of note, hyperphosphorylation of human cardiac titin at serine 12022 (serine 12884 in mice) has been identified in the human failing hearts (26). The PEVK spring element is the critical site of PRKCA's involvement in passive myocardial stiffness. PRKCA-mediated phosphorylation at serine decreases persistence length of the PEVK spring element, thus increasing the passive tension of skinned myocytes from mouse and pig hearts (27,28). Importantly, hyperglycemia can increase the gene and protein level of PRKCA in experimental diabetic pig and rat hearts (37,38), which is in line with the increased cardiac PRKCA in diabetic SKO mice. Second, changes in collagen content, geometry, and composition are associated with abnormal diastolic function and frequently seen in human HFpEF myocardium (25,29). The cardiac collagen deposition was elevated in SKO mice from a young age and increased with aging, in association with progressive diastolic dysfunction. In SKO myocardium, interstitial fibrosis was accompanied by activation of cardiac fibroblasts, consistent with human patients. In HFpEF patients, fibroblasts are presumed to convert to collagen-producing myofibroblasts because of exposure to TGF beta family and myocardial inflammation (39), both of which were elevated in SKO myocardium. Subsequently, we sought the underlying basis for increased inflammatory and fibrotic damage in the SKO mouse hearts. We observed massive neutrophil infiltration as well as NET formation in SKO myocardium. Hyperglycemia triggers oxidative stress of neutrophils and directly primes neutrophils to undergo NET and thereby contributes to diabetic retinopathy (40) and impaired wound healing (41). NET-derived components stimulate human pulmonary fibroblasts to myofibroblasts with elevated ACTA2 expression (42). The cytotoxic histone and deoxyribonucleic acid bound to NET induces organ fibrosis in aged mice (43). In addition, NET license macrophages to turn on transcriptional

TABLE 1 The Clinical Characteristics of Patients With Lean Diabetic HFpEF and Age-Matched Control Subjects Without HF

	Control Subjects (n = 291)	Lean Diabetic HFpEF (n = 291)	p Value
Demographics			
Age, years	67.2 ± 7.2	71.3 ± 10.4	<0.001
Women	133 (46)	137 (47)	0.740
NYHA functional class			<0.001
I	283 (98)	43 (16)	
II	7 (2)	160 (58)	
III	0 (0)	64 (23)	
IV	0 (0)	7 (3)	
Reduction in exercise tolerance	8 (3)	195 (67)	<0.001
Systolic BP, mm Hg	138 ± 20	134 ± 24	0.042
Body mass index, kg/m^2	24 ± 3.8	25 ± 3.0	0.020
Diabetes	33 (12)	291 (100)	<0.001
LV dimensions			
LVEDV, ml	83 (70, 101)	86 (66, 116)	0.27
IVSD, mm	9.0 (8.0, 10.0)	11.0 (9.0, 12.0)	<0.001
PWTD, mm	9.0 (8.0, 10.0)	10.0 (9.0, 12.0)	<0.001
LVMASS, g	142 (117, 170)	182 (141, 216)	<0.001
LVMASSi, g/m^2	85 (74, 101)	105 (88, 131)	<0.001
RWT	0.37 (0.33, 0.43)	0.44 (0.38, 0.52)	<0.001
LAVi, ml/m^2	28 (24, 32)	34 (25, 46)	<0.001
LVEF, %	64 (62, 67)	60 (55, 65)	<0.001
Diastolic function			
E wave, cm/s	66 (56, 77)	83 (66, 107)	<0.001
A wave, cm/s	75 (61, 85)	85 (69, 99)	<0.001
E medial, cm/s	6.0 (5.0, 7.1)	5.0 (4.0, 6.0)	<0.001
E/e′ medial	11 (8.8, 13)	17 (13, 22)	<0.001
E/e′ lateral	8.5 (6.8, 11)	12 (9.1, 16)	<0.001

Values are mean ± SD, median (interquartile range), or n (%). Depending on the types of data, Student's *t*-test, Wilcoxon rank sum test, or chi-square test for unpaired observations was applied and p values < 0.05 indicate statistical significance.

BP = blood pressure; HFpEF = heart failure with preserved ejection fraction; IVSD = interventricular septal thickness in diastole; LAVi = left atrial volume indexed to body surface area; LVEDV = left ventricular end-diastolic volume; LVEF = left ventricular ejection fraction; LVMASS = left ventricular mass; LVMASSi = LV mass indexed to body surface area; NYHA = New York Heart Association; PWTD = posterior wall thickness in diastole; RWT = relative wall thickness.

FIGURE 6 The SKO Mouse Is a Lean Diabetic Murine Model of HFpEF

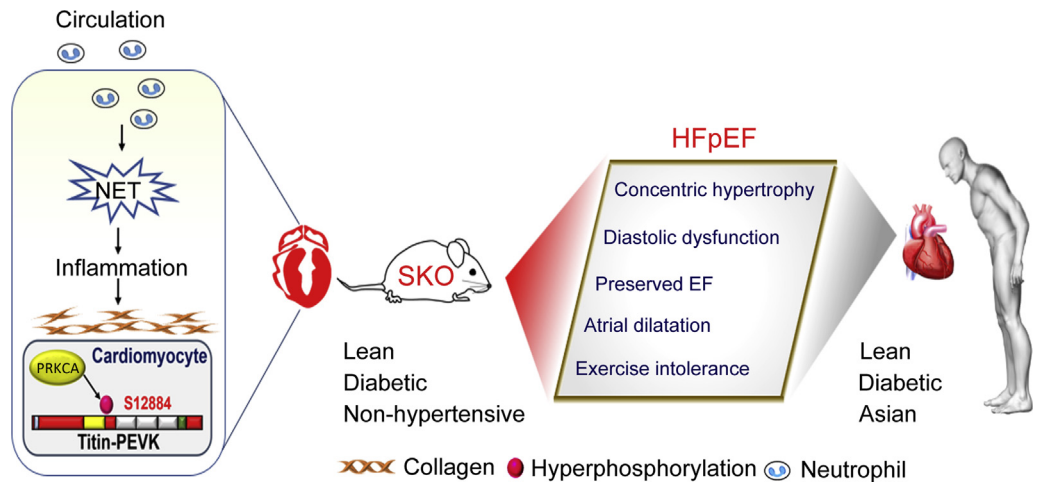

The lean diabetic SKO mice recapitulate major clinical manifestations of heart failure with preserved ejection fraction (HFpEF), resembling those observed in Asian populations, including LV concentric hypertrophy with preserved EF, increased left ventricular stiffness, and LA dilatation associated with exercise intolerance. Both cellular (PRKCA-mediated hyperphosphorylation of titin at the PEVK spring elements) and extracellular (reactive interstitial fibrosis) changes lead to left ventricular stiffness, and the latter is associated with massive neutrophil infiltration and neutrophil extracellular traps (NET) in mouse heart tissues. The NET, cellular titin changes, and extracellular interstitial fibrosis could be suggested as potential therapeutic targets in Asian HFpEF patients. Abbreviations as in **Figures 1, 2, and 4**.

regulation of *Il6* via toll-like receptor 2/4 in atherosclerosis (44). In the myocardium, the cytokines further amplify their actions primarily through the activation of JAK-STAT3 signaling. STAT3 is a ubiquitous stress-activated transcription factor that regulates gene programs important for hypertrophy, fibrosis, and inflammation (45). On cytokine binding to the specific receptors, STAT3 is phosphorylated and activated by JAK2 and then plays a crucial role in the induction of hypertrophic genes (21,22,46). Our findings show that SKO mice have cardiac inflammation, along with activated STAT3 signaling and induction of *Nppa* and *Acta1*, thus supporting the current recognition that comorbidity-driven inflammation contributes to the cardiac hypertrophy and adverse outcomes (47). As such, we suggest that NET may be a potential therapeutic target to intervene in inflammatory and fibrotic damage of SKO hearts. The activated peptidyl arginine deiminase 4 (PADI4) promotes citrullination of histone and allows decondensation of chromatin, a critical step for NET formation (33). PADI4 inhibitor (Cl-amidine) blocks NET formation and is successfully used to reduce atherosclerosis burden (48) and rescue wound healing in diabetic mice (49). It is of significant interest to examine whether Cl-amidine treatment produces beneficial effects on our HFpEF mice in a future study.

SKO MOUSE IS A UNIQUE LEAN DIABETIC HFpEF MODEL. An important benefit of preclinical animal models is the possibility to examine the contribution of single comorbidity in isolation without confounding risk factors, unlike clinical HFpEF patients frequently bound with multiple comorbidities. In terms of diabetic HFpEF models, so far, *db/db* mice with leptin receptor deficiency have been proposed to recapitulate multiple characteristics of clinical HFpEF (10,50). However, some phenotypic differences between obese diabetic *db/db* mice and lean diabetic SKO mice exist. Despite the presence of diastolic dysfunction, adult *db/db* mice develop mild LV hypertrophy, with only ~15% higher LV mass than in wild-type mice. Of note, adult *db/db* mice have apparent LV dilatation, distinct from SKO mice. The *db/db* mice also show evidence of cardiac fibrosis, but cardiac fibroblast of *db/db* mice does not undergo myofibroblast conversion (50). Another lean diabetic, nonhypertensive rat model induced by streptozotocin also shows diastolic dysfunction with increased ventricular stiffness as well as cardiac fibrosis. However, the LV eccentric hypertrophy and impaired contractile performance represent the major disadvantages

of this animal model for lean diabetic HFpEF study (51). Goto-Kakizaki rats display type 2 diabetes, salt-sensitive hypertension, hypertrophic cardiomyopathy, and cardiac fibrosis (52). However, there is little evidence that Goto-Kakizaki rat may be a lean diabetic HFpEF model. It is likely that the etiological and pathophysiological pathways are diverse among these preclinical models, despite some common clinical HFpEF features shared by animals. Thus, the specific animal model may only resemble a certain proportion of HFpEF patients. It is therefore important to carefully select suitable preclinical models for mechanistic investigation and therapeutic validation.

SKO MODEL IS CLINICALLY RELEVANT TO LEAN DIABETIC HFpEF PATIENTS IN ASIA. We believe that the current study is of particular relevance to Asian populations, in that "pure" metabolic disturbances of diabetes, without hypertension or obesity, may produce the HFpEF characteristics. The pan-Asian prospective study demonstrates that lean diabetic HFpEF patients, compared with other HF groups, have the worst quality of life, more severe signs and symptoms of HF, and the highest rate of the primary combined outcome of death and HF hospitalization (8). We further found that of 2,051 Asian patients with both body mass index and waist measurements, there was an inverse relationship between body mass index and risk of the composite outcome ("obesity paradox"); in contrast there was a direct relationship between waist-to-height ratio and risk of the composite outcome, suggesting that visceral adiposity plays an important role. The lean-fat (low body mass index but high waist-to-height ratio) patients had the highest proportion of diabetes associated with greater truncal obesity with overall sarcopenia (unpublished data presented at the ESC Heart failure Congress 2018), reminiscent of our lipodystrophic diabetic mouse model.

Moreover, the SKO model with uncontrolled hyperglycemia is clinically relevant, and appropriately represents the true natural history of diabetic HFpEF patients. Diabetic cardiomyopathy can manifest itself either as a restrictive phenotype with HFpEF or as a dilated phenotype with HF with reduced EF. The HFpEF phenotype is very common and usually occurs in patients with type 2 diabetes mellitus, whereas dilated cardiomyopathy is rare, is mainly observed in patients with type 1 diabetes mellitus. Accordingly, hyperglycemia, hyperinsulinemia, and lipotoxicity may predispose more to the HFpEF characteristics, while autoimmune processes rather lead to the HF with reduced EF features (53,54). In clinical HFpEF patients, the prevailing hypothesis is that hyperglycemia triggers a systemic inflammatory state that results in coronary microvascular endothelial dysfunction, which alters paracrine signaling between endothelial cells and cardiomyocytes and allows leukocytes to infiltrate the myocardium (5), contributing to cardiomyocyte stiffness and hypertrophy. Leukocyte infiltration leads to activation of myofibroblasts and interstitial collagen deposition. This is particularly so in the presence of hyperglycemia because cardiac PRKC activity is specifically augmented with hyperglycemia, thus promoting collagen production and deposition (55). These characteristics are clearly evident in the current SKO mice. Taken together, our SKO model represents a novel and validated murine model with lean diabetic HFpEF, which will bridge the large translation gap between preclinical and clinical studies and help to provide the more insightful understanding of the pathogenesis of the disease.

STUDY LIMITATIONS. This study provides a validated murine model of lean diabetic HFpEF and identifies underlying mechanisms. However, there remain several limitations. The inherent lipodystrophic phenotype of animals does not completely mimic the full spectrum of Asian patients' characteristics. The functional consequences of multiple titin phosphosites in the HFpEF mouse hearts remain unknown, and these consequences will likely be the subject of future studies. Moreover, despite the evidence supporting NET with pleiotropic effects to induce inflammation and tissue fibrosis, it remains to be conclusively demonstrated that NET are the primary mechanism by which diabetic conditions cause cardiac inflammation and fibrosis.

CONCLUSIONS

The lean diabetic SKO mice recapitulate major clinical manifestations of Asian HFpEF patients. Our findings help to clarify that diabetes, in the absence of obesity or hypertension, produces multiple HFpEF characteristics. Both cellular (PRKCA-mediated hyperphosphorylation of titin at the PEVK spring elements) and extracellular (reactive interstitial fibrosis) changes may lead to left ventricular stiffness, and the latter is associated with massive neutrophil infiltration and NET. The NET, cellular titin changes, and extracellular interstitial fibrosis may be potential therapeutic targets in Asian HFpEF patients.

ACKNOWLEDGMENTS The authors are grateful to their laboratory members and acknowledge the support from Singapore Bioimaging Consortium; Agency for Science, Technology and Research; and State Key Laboratory of Pharmaceutical Biotechnology and

Department of Pharmacology and Pharmacy, The University of Hong Kong. The authors also thank the Singapore Bioimaging Consortium-Nikon Imaging Center for support on microscopy. The contribution of all the site investigators and clinical coordinators of ASIAN-HF and ATTRaCT are acknowledged.

ADDRESS FOR CORRESPONDENCE: Dr. Yu Wang, Department of Pharmacology and Pharmacy, The University of Hong Kong, Sassoon Road 21, Hong Kong, China. E-mail: yuwanghk@hku.hk. OR Dr. Weiping Han, Singapore Bioimaging Consortium, Agency for Science, Technology and Research, 11 Biopolis Way, Singapore. E-mail: wh10@cornell.edu. OR Dr. Carolyn S.P. Lam, National Heart Centre Singapore and Duke-National University of Singapore, 5 Hospital Drive, Singapore. E-mail: carolyn.lam@duke-nus.edu.sg.

PERSPECTIVES

COMPETENCY IN MEDICAL KNOWLEDGE: Lean diabetes can produce the HFpEF characteristics, which is likely dependent on changed titin homeostasis and extracellular matrix fibrillar collagen. Both mechanisms are commonly identified in HFpEF animals and patients, suggesting that these could be potential therapeutic targets for HFpEF, despite the clinical etiologic heterogeneity.

TRANSLATIONAL OUTLOOK: Future research should test whether inhibition of neutrophil-induced myocardial inflammation and structural derangements can achieve therapeutic improvement for lean diabetic HFpEF in preclinical models and cohort studies.

REFERENCES

1. Lam CS, Pieske B. Heart failure with preserved ejection fraction (HFPEF) currently represents one of the greatest unmet needs in cardiology: introduction. Heart Fail Clin 2014;10:xv.

2. Owan TE, Hodge DO, Herges RM, Jacobsen SJ, Roger VL, Redfield MM. Trends in prevalence and outcome of heart failure with preserved ejection fraction. N Engl J Med 2006;355:251–9.

3. Yancy CW, Jessup M, Bozkurt B, et al. 2013 ACCF/AHA guideline for the management of heart failure: a report of the American College of Cardiology Foundation/American Heart Association Task Force on Practice Guidelines. J Am Coll Cardiol 2013;62:e147–239.

4. Shah SJ, Kitzman DW, Borlaug BA, et al. Phenotype-specific treatment of heart failure with preserved ejection fraction: a multiorgan roadmap. Circulation 2016;134:73–90.

5. Paulus WJ, Tschope C. A novel paradigm for heart failure with preserved ejection fraction: comorbidities drive myocardial dysfunction and remodeling through coronary microvascular endothelial inflammation. J Am Coll Cardiol 2013;62:263–71.

6. Tromp J, Teng TH, Tay WT, et al. Heart failure with preserved ejection fraction in Asia. Eur J Heart Fail 2018:1–14.

7. Bank IEM, Gijsberts CM, Teng THK, et al. Prevalence and clinical significance of diabetes in Asian versus white patients with heart failure. J Am Coll Cardiol HF 2017;5:14–24.

8. Tromp J, Tay WT, Ouwerkerk W, et al. Multimorbidity in patients with heart failure from 11 Asian regions: a prospective cohort study using the ASIAN-HF registry. PLoS Med 2018;15:e1002541.

9. Roh J, Houstis N, Rosenzweig A. Why don't we have proven treatments for HFpEF? Circ Res 2017;120:1243–5.

10. Valero-Munoz M, Backman W, Sam F. Murine models of heart failure with preserved ejection fraction: a "fishing expedition". J Am Coll Cardiol Basic Trans Science 2017;2:770–89.

11. Garg A. Acquired and inherited lipodystrophies. N Engl J Med 2004;350:1220–34.

12. Joffe BI, Panz VR, Raal FJ. From lipodystrophy syndromes to diabetes mellitus. Lancet 2001;357:1379–81.

13. Lupsa BC, Sachdev V, Lungu AO, Rosing DR, Gorden P. Cardiomyopathy in congenital and acquired generalized lipodystrophy: a clinical assessment. Medicine (Baltimore) 2010;89:245–50.

14. Sanon VP, Handelsman Y, Pham SV, Chilton R. Cardiac manifestations of congenital generalized lipodystrophy. Clin Diabetes 2016;34:181–6.

15. Nelson MD, Victor RG, Szczepaniak EW, Simha V, Garg A, Szczepaniak LS. Cardiac steatosis and left ventricular hypertrophy in patients with generalized lipodystrophy as determined by magnetic resonance spectroscopy and imaging. Am J Cardiol 2013;112:1019–24.

16. Wee K, Yang W, Sugii S, Han W. Towards a mechanistic understanding of lipodystrophy and seipin functions. Biosci Rep 2014;34:e00141.

17. McIlroy GD, Suchacki K, Roelofs AJ, et al. Adipose specific disruption of seipin causes early-onset generalised lipodystrophy and altered fuel utilisation without severe metabolic disease. Mol Metab 2018;10:55–65.

18. Lam CS, Anand I, Zhang S, et al. Asian Sudden Cardiac Death in Heart Failure (ASIAN-HF) registry. Eur J Heart Fail 2013;15:928–36.

19. Lam CS, Teng TK, Tay WT, et al. Regional and ethnic differences among patients with heart failure in Asia: the Asian sudden cardiac death in heart failure registry. Eur Heart J 2016;37:3141–53.

20. Heymans S, Corsten MF, Verhesen W, et al. Macrophage microRNA-155 promotes cardiac hypertrophy and failure. Circulation 2013;128:1420–32.

21. Kunisada K, Negoro S, Tone E, et al. Signal transducer and activator of transcription 3 in the heart transduces not only a hypertrophic signal but a protective signal against doxorubicin-induced cardiomyopathy. Proc Natl Acad Sci U S A 2000;97:315–9.

22. Kunisada K, Tone E, Fujio Y, Matsui H, Yamauchi-Takihara K, Kishimoto T. Activation of gp130 transduces hypertrophic signals via STAT3 in cardiac myocytes. Circulation 1998;98:346–52.

23. Yue H, Li W, Desnoyer R, Karnik SS. Role of nuclear unphosphorylated STAT3 in angiotensin II type 1 receptor-induced cardiac hypertrophy. Cardiovasc Res 2010;85:90–9.

24. Arnlov J, Ingelsson E, Riserus U, Andren B, Lind L. Myocardial performance index, a Doppler-derived index of global left ventricular function, predicts congestive heart failure in elderly men. Eur Heart J 2004;25:2220–5.

25. Zile MR, Baicu CF, Ikonomidis JS, et al. Myocardial stiffness in patients with heart failure and a preserved ejection fraction: contributions of collagen and titin. Circulation 2015;131:1247–59.

26. Hamdani N, Krysiak J, Kreusser MM, et al. Crucial role for Ca2(+)/calmodulin-dependent protein kinase-II in regulating diastolic stress of normal and failing hearts via titin phosphorylation. Circ Res 2013;112:664–74.

27. Hidalgo C, Hudson B, Bogomolovas J, et al. PKC phosphorylation of titin's PEVK element: a novel and conserved pathway for modulating myocardial stiffness. Circ Res 2009;105:631–8.

28. Hudson BD, Hidalgo CG, Gotthardt M, Granzier HL. Excision of titin's cardiac PEVK spring element abolishes PKC alpha-induced increases in

myocardial stiffness. J Mol Cell Cardiol 2010;48:972–8.

29. Rommel KP, von Roeder M, Latuscynski K, et al. Extracellular volume fraction for characterization of patients with heart failure and preserved ejection fraction. J Am Coll Cardiol 2016;67:1815–25.

30. Arora PD, McCulloch CA. Dependence of collagen remodelling on alpha-smooth muscle actin expression by fibroblasts. J Cell Physiol 1994;159:161–75.

31. Zeisberg EM, Kalluri R. Origins of cardiac fibroblasts. Circ Res 2010;107:1304–12.

32. Brinkmann V, Reichard U, Goosmann C, et al. Neutrophil extracellular traps kill bacteria. Science 2004;303:1532–5.

33. Lewis HD, Liddle J, Coote JE, et al. Inhibition of PAD4 activity is sufficient to disrupt mouse and human NET formation. Nat Chem Biol 2015;11:189–91.

34. Chin CW, Semple S, Malley T, et al. Optimization and comparison of myocardial T1 techniques at 3T in patients with aortic stenosis. Eur Heart J Cardiovasc Imaging 2014;15:556–65.

35. Dabir D, Child N, Kalra A, et al. Reference values for healthy human myocardium using a T1 mapping methodology: results from the International T1 Multicenter cardiovascular magnetic resonance study. J Cardiovasc Magn Reson 2014;16:69.

36. Linke WA, Hamdani N. Gigantic business: titin properties and function through thick and thin. Circ Res 2014;114:1052–68.

37. Guo M, Wu MH, Korompai F, Yuan SY. Upregulation of PKC genes and isozymes in cardiovascular tissues during early stages of experimental diabetes. Physiol Genomics 2003;12:139–46.

38. Giles TD, Ouyang J, Kerut EK, et al. Changes in protein kinase C in early cardiomyopathy and in gracilis muscle in the BB/Wor diabetic rat. Am J Physiol 1998;274:H295–307.

39. Westermann D, Lindner D, Kasner M, et al. Cardiac inflammation contributes to changes in the extracellular matrix in patients with heart failure and normal ejection fraction. Circ Heart Fail 2011;4:44–52.

40. Wang L, Zhou X, Yin Y, Mai Y, Wang D, Zhang X. Hyperglycemia induces neutrophil extracellular traps formation through an NADPH oxidase-dependent pathway in diabetic retinopathy. Front Immunol 2018;9:3076.

41. Wong SL, Demers M, Martinod K, et al. Diabetes primes neutrophils to undergo NETosis, which impairs wound healing. Nat Med 2015;21:815–9.

42. Chrysanthopoulou A, Mitroulis I, Apostolidou E, et al. Neutrophil extracellular traps promote differentiation and function of fibroblasts. J Pathol 2014;233:294–307.

43. Martinod K, Witsch T, Erpenbeck L, et al. Peptidylarginine deiminase 4 promotes age-related organ fibrosis. J Exp Med 2017;214:439–58.

44. Warnatsch A, Ioannou M, Wang Q, Papayannopoulos V. Inflammation: neutrophil extracellular traps license macrophages for cytokine production in atherosclerosis. Science 2015;349:316–20.

45. Haghikia A, Ricke-Hoch M, Stapel B, Gorst I, Hilfiker-Kleiner D. STAT3, a key regulator of cell-to-cell communication in the heart. Cardiovasc Res 2014;102:281–9.

46. Mir SA, Chatterjee A, Mitra A, Pathak K, Mahata SK, Sarkar S. Inhibition of signal transducer and activator of transcription 3 (STAT3) attenuates interleukin-6 (IL-6)-induced collagen synthesis and resultant hypertrophy in rat heart. J Biol Chem 2012;287:2666–77.

47. Borlaug BA. The pathophysiology of heart failure with preserved ejection fraction. Nat Rev Cardiol 2014;11:507–15.

48. Knight JS, Luo W, O'Dell AA, et al. Peptidylarginine deiminase inhibition reduces vascular damage and modulates innate immune responses in murine models of atherosclerosis. Circ Res 2014;114:947–56.

49. Fadini GP, Menegazzo L, Rigato M, et al. NETosis delays diabetic wound healing in mice and humans. Diabetes 2016;65:1061–71.

50. Alex L, Russo I, Holoborodko V, Frangogiannis NG. Characterization of a mouse model of obesity-related fibrotic cardiomyopathy that recapitulates features of human heart failure with preserved ejection fraction. Am J Physiol Heart Circ Physiol 2018;315:H934–49.

51. Akula A, Kota MK, Gopisetty SG, et al. Biochemical, histological and echocardiographic changes during experimental cardiomyopathy in STZ-induced diabetic rats. Pharmacol Res 2003;48:429–35.

52. D'Souza A, Howarth FC, Yanni J, et al. Chronic effects of mild hyperglycemia on left ventricle transcriptional profile and structural remodelling in the spontaneously type 2 diabetic Goto-Kakizaki rat. Heart Fail Rev 2014;19:65–74.

53. Paulus WJ, Dal Canto E. Distinct myocardial targets for diabetes therapy in heart failure with preserved or reduced ejection fraction. J Am Coll Cardiol HF 2018;6:1–7.

54. Maack C, Lehrke M, Backs J, et al. Heart failure and diabetes: metabolic alterations and therapeutic interventions: a state-of-the-art review from the Translational Research Committee of the Heart Failure Association-European Society of Cardiology. Eur Heart J 2018;39:4243–54.

55. Asbun J, Villarreal FJ. The pathogenesis of myocardial fibrosis in the setting of diabetic cardiomyopathy. J Am Coll Cardiol 2006;47:693–700.

KEY WORDS fibrosis, heart failure with preserved ejection fraction, neutrophil, seipin, titin

APPENDIX For supplemental material, please see the online version of this paper.